Raman and surface-enhanced Raman spectroscopy investigation of vasopressin analogues containing 1-aminocyclohexane-1-carboxylic acid residue

ARTICLE *in* BIOPOLYMERS · OCTOBER 2006

Impact Factor: 2.39 · DOI: 10.1002/bip.20545 · Source: PubMed

4 AUTHORS, INCLUDING:

Edyta Proniewicz (de domo Podstawka)
AGH Univesrity of Science and Technology in K…
98 PUBLICATIONS **1,134** CITATIONS
SEE PROFILE

Leonard M. Proniewicz
Jagiellonian University
196 PUBLICATIONS **2,434** CITATIONS
SEE PROFILE

Edyta Podstawka[1]
Emilia Sikorska[2]
Leonard M. Proniewicz[3]
Bernard Lammek[2]
[1] *Laser Raman Laboratory, Regional Laboratory of Physicochemical Analysis and Structural Research, Jagiellonian University, Ingardena 3 Str., 30-060 Kraków, Poland*

[2] *Department of Chemistry, University of Gdańsk, Sobieskiego 18 Str., 80-952 Gdańsk, Poland*

[3] *Faculty of Chemistry, Chemical Physics Division, Jagiellonian University, Ingardena 3 Str., 30-060, Kraków, Poland*

Raman and Surface-Enhanced Raman Spectroscopy Investigation of Vasopressin Analogues Containing 1-Aminocyclohexane-1-Carboxylic Acid Residue

Received 28 September 2005; revised 22 May 2006; accepted 25 May 2006
Published online 1 June 2006 in Wiley InterScience (www.interscience.wiley.com). DOI 10.1002/bip.20545

Abstract: *In this work, Raman spectroscopy (RS) was employed to characterize molecular structures of [Arg^8]vasopressin (AVP) and its [Acc^2,D-Arg^8]AVP, [Acc^3]AVP, and [Cpa^1,Acc^3]AVP analogues. The RS band assignments have been proposed. To determine the mechanism of adsorption of the above-mentioned compounds adsorbed on a colloidal silver surface, surface-enhanced Raman spectra (SERS) were measured. The SERS spectra were used to determine relative proximity of the adsorbed functional groups of the investigated peptides and their orientation on the silver surface. The AVP and [Acc^3]AVP SERS spectra (Acc: 1-aminocyclohexane-1-carboxylic acid) show that the L-tyrosine (Tyr) lies far from the metal surface, whereas the [Cpa^1,Acc^3]AVP spectrum (Cpa: 1-mercaptocyclohexaneacetic acid) provides evidence that Tyr interacts with the silver surface. These results suggest the binding of the Tyr-ionized phenolic group might be responsible for the selectivity of the analogues. We show that the aromatic ring of L-phenylalanine (Phe) of AVP and [Acc^2,D-Arg^8]AVP interacts with the silver surface. The strength of this interaction is considerably weaker for [Acc^2,D-Arg^8]AVP than for AVP. This might be due either to a longer distance between the Phe ring and the silver surface, or to the almost perpendicular orientation of the Phe ring towards the surface. The carbonyl group of the L-glutamine acid (Gln) or L-asparagine acid (Asn) of AVP, [Acc^2,D-Arg^8]AVP, and [Acc^3]AVP is strongly bound to the silver*

Correspondence to: Bernard Lammek; e-mail: bernard@hebe.chem.univ.gda.pl or Leonard M. Proniewicz; e-mail: proniewi@chemia.uj.edu.pl

Contract grant sponsor: internal Jagiellonian University grant; contract grant number: WChUJ/DS/05/2004.

surface. We have also found that all peptides adsorb on the silver surface via sulfur atoms of the disulfide bridge, adopting a "GGG" conformation, except [Cpa[1],Acc[3]]AVP, which accepts a "TGG" geometry. Biopolymers 83: 193–203, 2006

This article was originally published online as an accepted preprint. The "Published Online" date corresponds to the preprint version. You can request a copy of the preprint by emailing the Biopolymers editorial office at biopolymers@wiley.com

Keywords: *[Arg[8]]vasopressin, AVP; [Arg[8]]vasopressin analogues; Raman spectroscopy, RS; surface enhanced Raman scattering, SERS*

INTRODUCTION

[Arg^8]vasopressin (AVP), a neurohypophyseal hormone, is a nonapeptide with a disulfide bridge between L-cysteine (Cys) at positions 1 and 6 (Cys–Tyr–Phe–Gln–Asn–Cys–Pro–Arg–Gly–NH_2). The –S–S– unit in this peptide consisting of a six-membered amino acid ring and a C-terminal amidated group produces a three-residue tail.[1]

AVP plays a primary role in the regulation of renal water excretion and a secondary role in the regulation of cardiovascular function in mammals. It is believed that Tyr at position 2 of the polypeptide (Tyr^2) chain of AVP initiates the pressor response of AVP, while Phe at position 3 (Phe^3) is involved mainly in the recognition of this hormone and its binding to receptors.[2] The interaction of AVP with its receptors is determined by appropriate orientations of Tyr^2 and Phe^3 of the side chains. The orientation of Tyr^2 and Phe^3 in [Arg^8]vasopressin is stabilized by a parallel π–π interaction between the aromatic rings of these residues. As a consequence, the side chains of both aromatic residues extend away from the cyclic moiety.[3] The earlier conformational studies of the native [Arg^8]vasopressin in aqueous[4,5] and DMSO[6] solutions using two-dimensional nuclear magnetic resonance (2D NMR) spectroscopy showed that its dominant structure is the β-turn structure within the Tyr^2–Asn^5 region. Similar results were obtained by computational studies of the AVP molecule in vacuum.[7,8] These results revealed two β-turns at positions 3,4 and 4,5. X-ray investigations of pressinoic acid also show type II′ and type I of the β-turns at positions 3,4 and 4,5, respectively.[9]

Raman spectroscopy is a very valuable technique for qualitative and quantitative measurements of different structural components and determination of the secondary structure of peptides and proteins. For instance, the frequencies and intensities of amide I and III bands in the Raman spectrum can be correlated with the specific secondary conformations of polypeptide chain in polypeptides and proteins.[10–13]

Surface-enhanced Raman scattering (SERS) is used for studying interactions between different compounds such as amino acids, peptides, etc., with metal surfaces. This is a very selective method that provides information about groups that directly interact with the metal surface or lie in close proximity to it.[14,15] Based on these specific interactions, the geometry of adsorbed species can be deduced. Further, this information may allow the proposition of a mechanism for a substrate binding to its receptor.

In our previous work, we found that the substitution of AVP at position 2 with 1-aminocyclohexane-1-carboxylic acid (Acc^2) results in a very potent agonist of V_2 receptors. This analogue also displays weak antiuterotonic and antipressor properties[16] In another analogue, Phe at position 3 was replaced with Acc. This modification caused the loss of agonism towards the OT receptors. The [Acc^3]AVP analogue exhibits only weak pressor and antidiuretic activities[16] and significantly reduced activities as compared to [Acc^2]AVP. An additional replacement at position 1 with 1-mercaptocylohexaneacetic acid in [Acc^3]AVP, i.e., [Cpa^1,Acc^3]AVP, allowed us to obtain the analogue, which, surprisingly, turned out to be a highly selective V_2 agonist.

AVP is an important biologically active molecule, in which substitution of Tyr^2 and/or Phe^3 in the peptide sequence changes its biological properties. This is why, using Raman spectroscopy (RS), we decide to investigate the structure of AVP and its modified analogues, listed above. Additionally, to understand AVP's structural changes upon chain modification and its structure–activity relationship, we used SERS.

EXPERIMENTAL

Peptide Samples

AVP was purchased from Bachem AG and used without further purification. Vasopressin analogues were synthesized according to the literature.[16] The purity and identity of each peptide was determined by high performance liquid chromatography (HPLC) and fat atom bombardment (FAB) mass spectrometry. The products were purified by HPLC partition chromatography using two solvent system*s*:

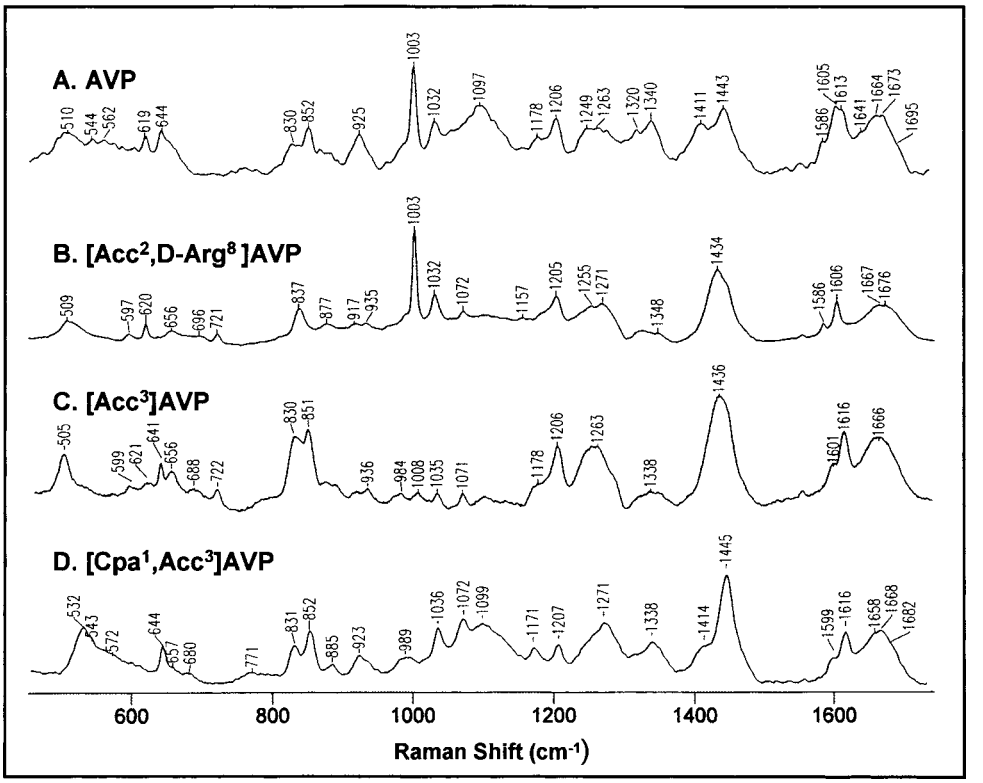

FIGURE 1 Raman spectra of (A) AVP, (B) [Acc^2,D-Arg^8]AVP, (C) [Acc^3]AVP, and (D) [Cpa^1, Acc^3]AVP.

0.1% aqueous trifluoroacetic acid (TFA) and acetonitrile:0.1 TFA (80:20 v/v), followed by Sephadex G-15 and LH-20 gel filtration.

Raman Spectroscopy

The Raman spectra of AVP and its analogues were obtained with a triple-grating spectrometer (Jobin Yvon, T 64000) equipped with a liquid-nitrogen-cooled charge-coupled device (CCD) detector (Jobin Yvon, model CCD3000). A spectral resolution of 4 cm^{-1} was set in these measurements. The 514.5-nm line of an Ar-ion laser (Spectra-Physics, model 2025) was used as the excitation source. Laser power at sample was set at 20 mW.

SERS Spectroscopy

$AgNO_3$ and $NaBH_4$ were purchased from Sigma-Aldrich Co. (Poznań, Poland) and used without further purification. Solutions of the colloidal silver were prepared according to a standard procedure.[17] To describe this process briefly: 8.5 mg of $AgNO_3$ dissolved in 50 mL of deionized water at 4°C was added dropwise to the 150 mL of 1 m*M* solution of $NaBH_4$, immersed in an ice bath stirred vigorously. Once the addition of $AgNO_3$ was completed, the resulting pale-yellow solution was stirred and maintained at 4°C for approximately 1 h. The excitation spectrum of the Ag sol prepared in this manner (pH ~ 8.3) had an absorbance maximum at 396 nm. Sample solutions were prepared by dissolving each of the investigated peptides in deionized water. The concentrations of the samples before mixing with the colloid were set at $10^{-4}M$. The final sample concentration in the silver colloid was $\sim 10^{-5}M$.

SERS spectra were obtained using the same equipment as for Raman spectra. No spectral changes due to the thermal degradation or desorption process were observed during these measurements.

Spectral Analysis

Second derivatives of Raman spectra, in the range of the amide I bands of [Arg^8]vasopressin (AVP) and its [Acc^2,D-Arg^8]AVP, [Acc^3]AVP, and [Cpa^1,Acc^3]AVP analogues were calculated with the derivative function (Sav-Golay) of the Grams/AI(7.0) program from Galactic (Galactic Industries Co., Salem, NH).

RESULTS AND DISCUSSION

Raman Studies

Figure 1 shows the Raman spectra of (A) AVP and its modified analogues (B) [Acc^2,D-Arg^8]AVP, (C) [Acc^3]AVP, and (D) [Cpa^1,Acc^3]AVP in the spectral range of 450–1750 cm^{-1}. The assignment to the normal coordinates of bands appearing in these spectra is proposed on the ground of the earlier studies on

Table I Frequencies and Band Assignments in the Raman Spectra of AVP and Its Analogues

	Frequency (cm^{-1})			
Assignment	AVP	[Acc^2,D-Arg^8] AVP	[Acc^3] AVP	[Cpa^1,Acc^3] AVP
Amide I	1695			
	1673	1676		1682
	1664	1667	1666	1668
	1641			1658
Tyr (ν_{8a})	1613		1616	1616
Phe (ν_{8a})	1605	1606	1601	
Tyr and/or Phe(ν_{8b})	1586	1586		1599
$\delta(CH_2)$	1443	1434	1436	1445
Gln and/or Asn ν(C=O)	1411			1414
δ(C—H)	1340	1348	1338	1338
δ(C—H)	1320	1323	1323	
Amide III	1263	1271	1263	1271
	1249	1255		
Tyr and/or Phe (ν_{7a})	1206	1205	1206	1207
Tyr and/or Phe (ν_{9a})	1178	1157	1178	1171
Gln and/or Asn $\rho_\tau(NH_2)$	1117	1120	1118	
			1071	1099
ν(C—N)	1097	1072	1035	1072
			1007	1036
Phe (ν_{18a})	1032	1032		
Phe (ν_{12})	1003	1003		
			984	
		935	936	989
ν(C—C)	925	917	922	923
		877	890	885
			877	
Tyr	852		851	852
	830		830	831
$\delta(CCC)_{\text{proline ring}}$ and/or ν_s (CCN)	839	837		
cyclohexane ring breathing				771
ν(C—S) P_C-T		721	722	
ν(C—S) P_C-G		696	688	680
ν(C—S) P_H-T	656	656	656	657
Tyr (ν_{6b})	644		641	644
Phe (ν_{6b})	619	620	621	
		597	599	
	562			572
ν(S—S) TGT	544			543
ν(S—S) TGG				532
ν(S—S) GGG	510	509	505	

oxytocin/vasopressin superfamily peptides[12,18–20] and other small proteins.[12,21–23] The band frequencies, together with their assignments, are summarized in Table I.

The Raman spectra presented in Figure 1 are dominated by spectral features due to the aromatic ring vibrations of the Phe and/or Tyr residues. Hence, the main differences between these spectra arise from the absence of either the Tyr or Phe modes. The AVP contains both the Tyr^2 and Phe^3 residues, while Phe^3 in the polypeptide chain of [Acc^3]AVP and [Cpa^1,Acc^3]AVP and Tyr^2 of [Acc^2,D-Arg^8]AVP are substituted by 1-aminocyclohexane-1-carboxylic acid. Thus, in the Raman spectra of the two former analogues enhancement of the Tyr vibrations is observed, whereas in the case of [Acc^2,D-Arg^8]AVP the Phe modes dominate the spectrum.

The most intense band at 1003 cm^{-1} in the AVP and [Acc^2,D-Arg^8]AVP Raman spectra (Figure 1A and 1B) corresponds to the symmetric "breathing"

vibrations (ν_{12}) of the phenyl ring. At the higher frequency side of this band, around 1032, 1178, 1206, 1586, and 1605 cm^{-1}, several characteristic Phe bands appear that are due to the "in-plane" CH bending (ν_{18a}), the combination of in-plane CH bending (ν_{9a}) with ring stretching, the phenyl-C stretching (ν_7), the "in-plane" CH stretching (ν_{8a}), and the in-plane ring stretching (ν_{8b}) vibrations, respectively. On the other hand, in the lower-frequency region of these spectra, only one Phe mode is enhanced at $\sim$619 cm^{-1}. It is due to the "in-plane" ring deformation vibrations (ν_{6b}).[23–25]

Among all Tyr characteristic bands, those at 830 and 850 cm^{-1}, so-called tyrosine doublet, are considered useful for determining the environment of the tyrosine side chain and for indicating whether tyrosine residue is "buried" or "exposed." If the Raman intensity of the 850-cm^{-1} band is greater than the intensity of the 830-cm^{-1} band, it is likely that the Tyr side chain is exposed to the environment, whereas if has a lower intensity, the Tyr side chain is either buried, or the tyrosine OH group becomes a hydrogen-bond donor.[25] In the case of the Raman spectra presented in this work, the Tyr doublet is observed at 830/852 cm^{-1} for AVP (Figure 1A) and around 830/851 cm^{-1} for [Acc^3]AVP and [Cpa^1,Acc^3]AVP (Figure 1C and 1D). The I_{850}/I_{830} intensity ratio for the above-mentioned peptides exceed 1, indicating that the phenolic oxygen acts as a much weaker proton donor, or as an acceptor to an external acidic proton.

Among a variety of interactions in peptides and proteins, formation of disulfide bridge(s) is very important for the protein folding. The Raman spectra yield excellent information about disulfide bond conformations, based on the frequency of the S—S and C—S stretching vibrations. The frequency of these vibrations allows the determination of the geometry of the —C—S—S—C— molecular fragment because the ν(S—S) depends on the dihedral angle around the C—S bond[25–27] in the vicinity of the S—S bridge, and also on the φ and ϕ torsion angles of the adjacent peptide groups.[28] Generally, it is accepted that the *gauche–gauche–gauche* (GGG) conformation gives rise to ν(S—S) observed near 510 cm^{-1},[12] while the *gauche–gauche–trans* (GGT) and *trans–gauche–trans* (TGT) rotamers are characterized by the 525- and 540-cm^{-1} bands, respectively.[25,26] Internal rotation along the C_α—C_β axis of Cys causes formations of various conformations of the C—S bond. Several of them are well established by their characteristic frequencies[27]: P_H-T, P_C-G, P_H-T, P_H-G, P_N-T, and P_N-G, where P_C, P_H, and P_N indicate three plausible conformations of the X—CH—CH_2—S moiety (X = H, C, or N) with the carbonyl carbon, H_α proton, and amide nitrogen at the *trans* position to the sulfur atom, respectively, whereas T and G refer to the *trans* or *gauche* conformation in relation to the C—S bond, i.e., to the torsion angle of 180°or 90°.[29]

Thus, the 510- and 544-cm^{-1} bands in the Raman spectrum of AVP (Figure 1A) due to the disulfide bridge stretching vibrations, ν(S—S), suggest the presence of two different conformations of the disulfide bridge GGG and TGT, respectively. Similarly, in the Raman spectrum of [Cpa^1,Acc^3]AVP, the two ν(S—S) band are found at 543 and 532 cm^{-1}. The former band arises from the TGT conformer, while the latter is due to the TGG rotamer. On the other hand, in the [Acc^2,D-Arg^8]AVP and [Acc^3]AVP Raman spectra, a single band around 505–509 cm^{-1} is enhanced. Its frequency points out that the —C—S—S—C— fragment in these peptides adopts the GGG geometry.

The bands of the 750–600-cm^{-1} region due to the stretching vibrations of the C—S bonds provide information about the C—C bonds adjacent to the C—S linkage. Thus, the $\sim$656-cm^{-1} band (see Table I for detailed frequencies) in all Raman spectra presented in Figure 1 is due to ν(C—S) of the P_H-T rotamer. The AVP shows only this one conformer of the —C—S— moiety (Figure 1A), whereas [Cpa^1,Acc^3]AVP shows one and [Acc^2,D-Arg^8]AVP and [Acc^3]AVP two additional rotamers. The 722- and 688-cm^{-1} bands in the [Acc^3]AVP spectrum (Figure 1C) and the 721- and 696-cm^{-1} bands in the [Acc^2,D-Arg^8]AVP spectrum (Figure 1B) characterize the P_C-T and P_H-G geometry of the —C–S– fragment, respectively. On the other hand, the frequency of ν(C—S) at 680 cm^{-1} for [Cpa^1,Acc^3]AVP (Figure 1D) indicates the presence of the P_H-G conformer.

Among all bands observed in the Raman spectra presented in this work, the amide I and III vibrations provide information about the secondary structure of the investigated peptides. Previous studies of the conformational properties of AVP using Raman spectroscopy showed that the major amide I and III bands appear at 1667 and 1274 cm^{-1}, respectively.[30] In addition, a shoulder on the amide I band at 1676 cm^{-1} was found. On the ground of these findings, the authors have excluded the possibility of an α-helical conformation in AVP.

The Raman spectrum of AVP presented in Figure 1A shows a broad complex envelope of the amide I bands, which consists of at least four components with frequencies at about 1641, 1664, 1673, and 1695 cm^{-1} (see Figure 1A). With no doubt, a maximum at 1664 cm^{-1} is due to the random-coil conformation, while the 1673-cm^{-1} band is assigned to the β-turn structure. The 1641- and 1695-cm^{-1} bands assignment

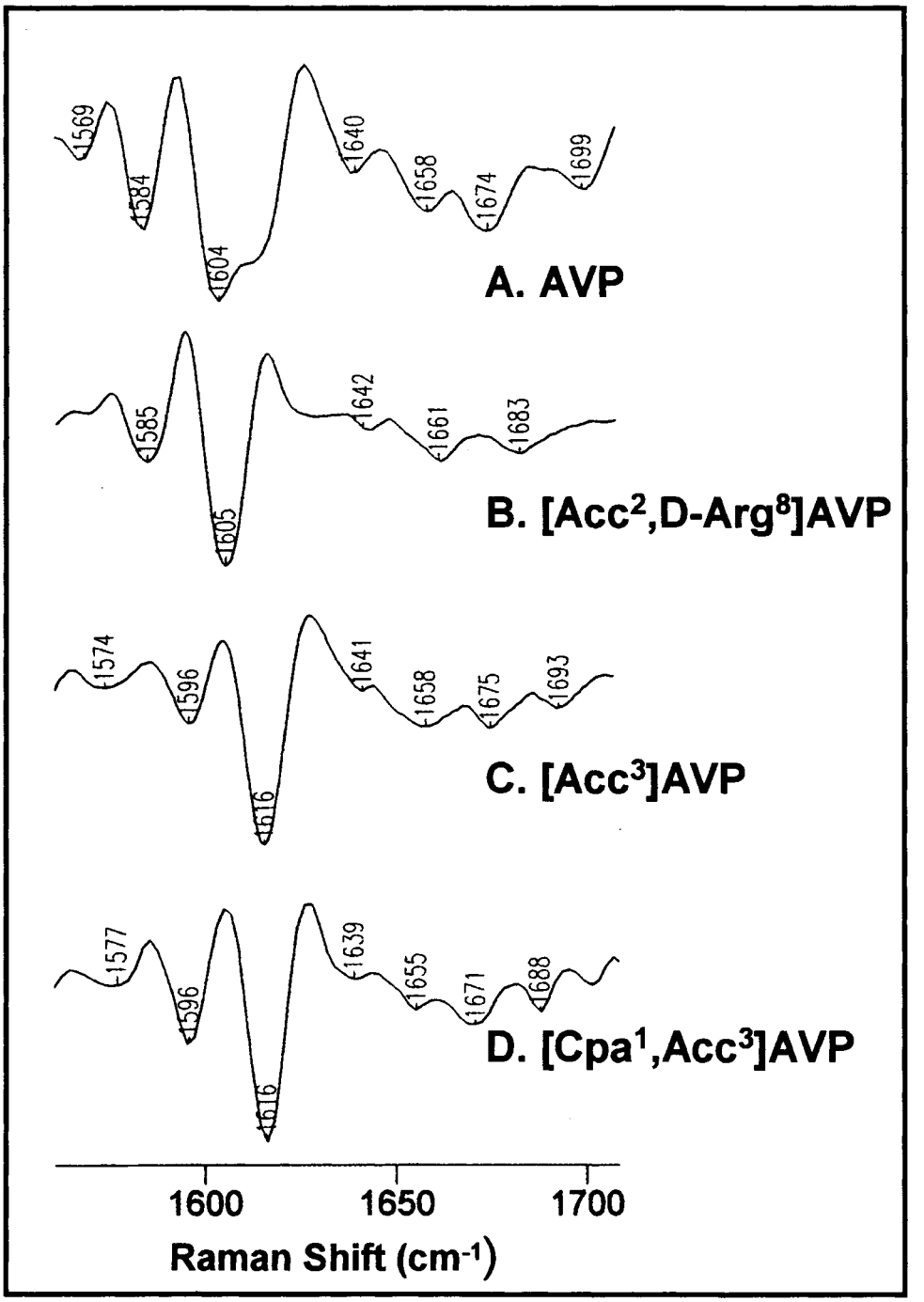

FIGURE 2 Second-derivative Raman spectra of (A) AVP, (B) [Acc^2,D-Arg^8]AVP, (C) [Acc^3]AVP, and (D) [Cpa^1,Acc^3]AVP.

to the β-sheet structure is clear also, because previous authors predicted no α-helical structure in the AVP.[4–6] To enhance the Raman spectra resolution, we have calculated the second-derivative Raman spectrum for AVP (see Figure 2A), which reveals four bands in the amide I range of 1640, 1658, 1674, and 1699 cm^{-1}. The assignments of the 1640- (β-sheet), 1674- (β-turn), and 1699-cm^{-1} (β-sheet) spectral feature are obvious[31–34]; further, they are in agreement with the allocation of these bands in the AVP Raman spectrum and with the earlier conformational investigations.[4–6,8,35–38] The remaining band, at 1658 cm^{-1}, has been assigned to the random-coil structure of strongly hydrogen-bonded amide bonds.[35]

Table II Calculated Frequencies of the Second-Derivative Raman Spectra with Their Allocation to the Conformational Structure

	Frequency (cm^{-1})			
Assignment	AVP	[Acc^2,D-Arg^8] AVP	[Acc^3] AVP	[Cpa^1,Acc^3] AVP
β-Sheet	1640	1642	1641	1639
Random coil	1658	1661	1685	1655
Turn	1674	1683	1675	1671
β-Sheet	1699		1693	1688

Similarly as in the case of AVP, the Raman spectra of [Acc^2,D-Arg^8]AVP, [Acc^3]AVP, and [Cpa^1, Acc^3]AVP in the frequency region of the amide I vibrations give a broad band with maxims at 1667 and 1676 cm^{-1}; 1666 cm^{-1}; 1658, 1668, and 1682 cm^{-1}, respectively. The calculated second-derivatives spectra reveal several overlapping bands in this range. Their frequencies, together with their assignments to the proper conformation, are summarized in Table II. In brief, the amide I band of [Cpa^1,Acc^3]AVP (Figure 2D) shows four components (1639 cm^{-1}, β-sheet; 1655 cm^{-1}, random-coil; and 1671 and 1688 cm^{-1}, β-turns), while [Acc^2,D-Arg^8]AVP (Figure 2B) shows three (1642 cm^{-1}, β-sheet; 1661 cm^{-1}, random-coil; and 1683 cm^{-1}, turn) and [Acc^3]AVP (Figure 2C) up to four components (1639 cm^{-1}, β-sheets; 1655 cm^{-1}, random-coil; 1671 cm^{-1}, turn; and 1688 cm^{-1}, β-sheet).

The prediction of the secondary structure for all the peptides investigated in this work, on the ground of the amide III band, is in agreement with the results obtained from the analysis of the amide I region.

Surface-Enhanced Raman Scattering Studies

Figure 3 presents the SERS spectra of all peptides investigated in this work. The SERS band assignment to the normal coordinates is proposed on the ground of the earlier studies on aliphatic and aromatic amino acids,[17,39,40] peptides,[27,41,42] and proteins[12,43,44] adsorbed on colloidal silver particles. The assignment, together with the observed band frequencies, is summarized in Table III.

In the SERS spectra, similar to those presented in Figure 1, the bands associated with the aromatic residues are dominant in the spectra. This supports a general observation that the aromatic rings show a liability for binding to the silver surface. It is also believed that

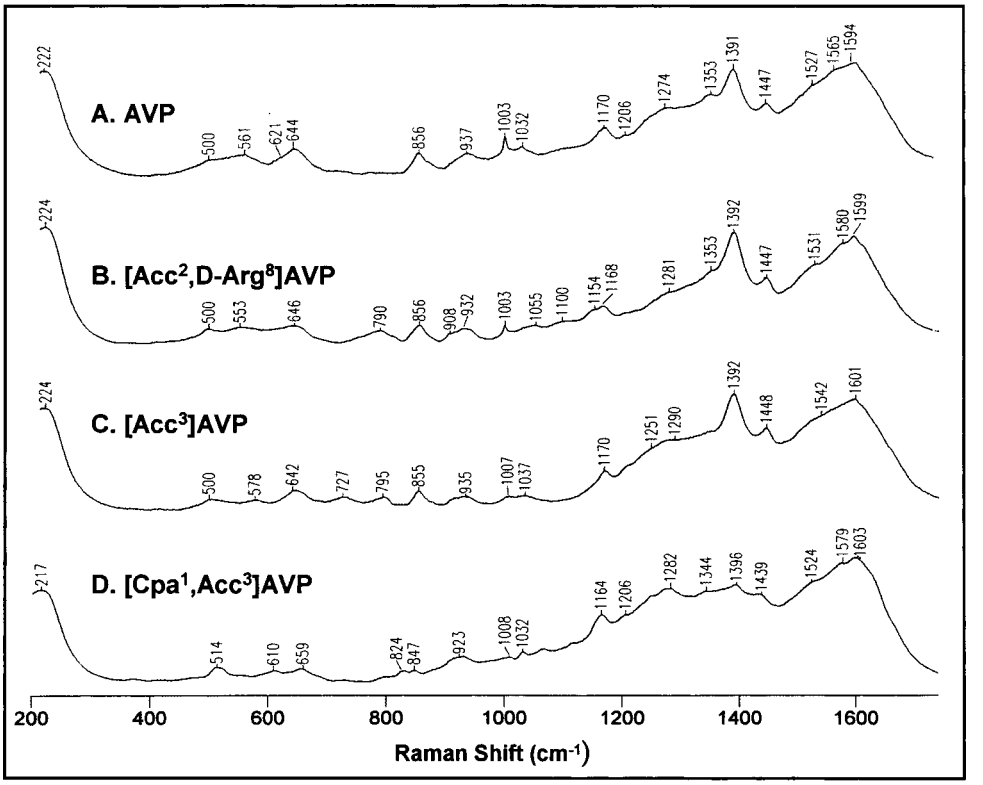

FIGURE 3 SERS spectra of (A) AVP, (B) [Acc^2,D-Arg^8]AVP, (C) [Acc^3]AVP, and (D) [Cpa^1,Acc^3]AVP.

Table III Frequency and Band Assignments for the SERS Spectra of AVP and Its Analogues

	Frequency (cm^{-1})			
Assignment	AVP	[Acc^2,D-Arg^8]AVP	[Acc^3]AVP	[Cpa^1,Acc^3]AVP
Tyr and/or Phe (ν_{8a})	1594	1599	1601	1603
Tyr, Phe (ν_{8b}), and/or ν_{as}(C=O) in Gln and/or Asn	1565	1580		1579
Amide II	1527	1531	1542	1524
$\delta(CH_2)$	1447	1447	1448	1439
ν_s(C=O) Gln and/or Asn	1391	1392	1392	1396
δ(C—H)	1353	1353		1344
Amide III and/or $\delta(CC_\alpha H)$	1274	1281	1290	1282
Phe or Tyr	1206			1206
Tyr and/or Phe (ν_{9a})	1170	1168	1170	1164
Gln and/or Asn $\rho_\tau(NH_2)$				1114
ν(C—N)		1054	1037	1065
				1032
$\nu_{as}(C_\alpha CN)$ and/or Phe (ν_{18a})	1032	1100 1031		
Tyr			1007	1008
Phe (ν_{12})	1003	1003		
ν(C—CO)	937	932	935	923
ν_s(CNC) secondary amide	856	856	855	
Tyr				847
				824
cyclohexane ring breathing		790	795	796
ν(C—S) P_C-T			727	
ν(C—S) P_H-T	644	646	642	659
Phe (ν_{6b}) and/or ν(C—S)P_H-G	621 561	553	578	
ν(S—S) TGG				514
ν(S—S) GGG	500	500	500	

the phenyl ring forms a complex between its π-electron system and the silver.[45] The formation of the complex is accompanied by broadening, increasing of intensity, and a slight lowering of the frequencies for the aromatic ring modes.[12] In the SERS spectra of AVP and [Acc^2,D-Arg^8]AVP (Figures 3A and 3B), we observed a down shift by a few wavenumbers (Δ = 2–8 cm^{-1}) of the ν_{8a} (1594–1599 cm^{-1}), ν_{8b} ($\sim$1580 cm^{-1}), and ν_{9a} ($\sim$1170 cm^{-1}) Phe modes, and their relatively strong intensity in comparison to the respective Raman spectra. The red shifting and broadening of these bands suggest a direct interaction of the Phe ring with the silver nanoparticles surface.[46] The other two Phe modes, i.e., ν_{12} and ν_{6b}, are barely observed in these spectra. The former band, at 1003 cm^{-1}, does not change its Raman frequency, but its intensity is dramatically reduced. However, the intensity of this band for AVP is still higher than that for [Acc^2,D-Arg^8]AVP, which suggests a different orientation of these peptides on the silver surface. The latter band overlaps with ν(C—S) and appears as a shoulder at 621 cm^{-1} for AVP only. The lack of the significant frequency shift and the low intensity of ν_{12} points out either that the Phe aromatic ring does not lie flat on the silver surface but rather adopts a tilted or perpendicular orientation to it, or that the Phe ring approaches the silver colloidal sphere but does not adsorb on it.[47,48] Again, the analysis of the intensity of this band for AVP and [Acc^2,D-Arg^8]AVP suggests, according to the surface selection rules,[49] that the angle between the Phe ring and the surface is greater for [Acc^2,D-Arg^8]AVP than for AVP.

In the SERS spectra of AVP and its Tyr^2 analogues, i.e., [Acc^3]AVP and [Cpa^1,Acc^3]AVP, the Tyr ring vibrations are also enhanced. Characteristic vibrations at around 1601, 1579, and 1164–1170 cm^{-1} are observed. The 1601- and 1579-cm^{-1} spectral features overlap

with other bands in this region, such as the amide I and II vibrations (amide II vibrations are enhanced in the SERS spectra thanks to the molecular reorientation and the changes in the component of the local field upon adsorption on the metal surface), as well as the C=O asymmetric stretching and NH_2 deformation vibrations. In the case of AVP, the Tyr modes are hidden additionally under the Phe modes. It is worth pointing out that the tyrosine doublet is observed only in the case of [Cpa^1,Acc^3]AVP. It appears at 824/847 cm^{-1}. This phenomenon suggests that only [Cpa^1,Acc^3]AVP binds to the silver surface through the phenolic oxygen atom after a loss of the hydrogen atom. The SERS intensities of these bands are nearly equal, thus indicating that the hydroxyl group of the side chain is ionized. Additionally, the normal mode analysis for a *para*-substituted benzene provides evidence that vibrations with strong components of atomic motion perpendicular to the surface receive the most enhancement.[48–50] Thus, the appearance of the strong 1603- and 1165-cm^{-1} bands confirms the ionization of the Tyr hydroxyl group. Also, the relatively weak intensity of the Tyr doublet in the SERS spectrum of [Cpa^1,Acc^3]AVP in comparison to the corresponding Raman spectrum indicates that Tyr either weakly adsorbs on the silver surface or adopts a tilted geometry on the surface.

The analysis of the SERS spectra shows that the disulfide bridge of each investigated peptide is involved in the adsorption process as well. The enhancement of a single band at 500 cm^{-1} in the SERS spectra of AVP, [Acc^2,D-Arg^8]AVP, and [Acc^3]AVP (GGG geometry) and at 514 cm^{-1} for [Cpa^1,Acc^3]AVP (TGG geometry) due to stretching vibrations of the S—S bond indicates that this bond interacts with the silver surface through lone electron pairs of the sulfur atoms without its cleavage. The intensities of these SERS bands are weak. Additionally, the frequencies of these bands are down shifted by about 10 cm^{-1} in comparison to the frequencies of the corresponding Raman bands. These phenomena may point out that the S—S bond, in all peptides investigated here, is in close proximity to the silver surface. However, the observed small shift in the frequency in comparison to Raman spectrum may be also due to small changes in the S—S bond conformation that are induced by the weak interaction with metal surface.

The slightly lower SERS intensity of the ν(S—S) band for each of peptides investigated here as compared to their Raman intensities suggests that in all cases the S—S bridge does not cleave upon adsorption but adopts a tilted orientation on the silver surface. However, it seems that the enhancement of the ν(S—S) band in the SERS spectrum of [Cpa^1,Acc^3]AVP is slightly stronger than that in the other three cases. This fact may be explained by a stronger interaction between the sulfur atom(s) and the silver surface and by weakening of the S—S bond for this analog. On the other hand, Yim et al. proposed two different orientations of the S—CH_3 bond, almost parallel (named α) and tilted (named β), on the silver surface.[51] The authors showed that for almost parallel orientation of the S—CH_3 bond on the surface ν(S—CH_3), which is expected to has a large polarizability derivative component along the bond direction, cannot be strongly enhanced compared to other modes, while for the β-type orientation this vibration is more enhanced.[52] By analogy, we imply that stronger enhancement of ν(S—S) for [Cpa^1,Acc^3]AVP adsorbed on the silver surface suggests that the angle between the S—S bond in this peptide assumes a higher degree value in comparison to other analogues.

The participation of the disulfide bridge in the peptide adsorption process on the silver surface influences the conformation of the atoms adjacent to the S—S bond. This is why a careful analysis of the 600–750-cm^{-1}spectral region is needed. The $\sim$645-cm^{-1} band for AVP and [Acc^2,D-Arg^8]AVP, the 642-cm^{-1} band for [Acc^3]AVP, and the 659-cm^{-1} band observed in the SERS spectrum of [Cpa^1,Acc^3]AVP characterizes the P_H-T rotamer of the —C—C—S—S— fragment. Only one of these peptides, namely [Acc^3]AVP, exhibits the additional P_C-T conformer of the above-mentioned molecular fragment that is characterized by the 727-cm^{-1} band. All these observed ν(C—S) frequencies are slightly down shifted due to the withdrawal of the electron density from the C—S bond upon the binding of the sulfur atom to the silver surface.[28] A comparison of these findings with the results of the Raman spectra analysis shows that only AVP does not change its —C—C—S—S— conformation upon deposition on the colloidal silver surface. A different behavior is observed in the other three cases. The SERS spectra of [Acc^2,D-Arg^8]AVP, [Acc^3]AVP, and [Cpa^1,Acc^3]AVP show a lower number of the ν(C—S) vibrations, due to the lower number of rotamers, in comparison with the Raman spectra. This indicates that these peptides have a more rigid structure in the presence of the silver colloid surface than in the solid phase.

A common spectral feature, observed in the all SERS spectra presented in Figure 3, is the 1391–1396-cm^{-1} band due to the C=O stretching vibrations, ν(C=O). The intensity of this band in the SERS spectra of AVP, [Acc^2,D-Arg^8]AVP, and [Acc^3]AVP is strong, while for [Cpa^1,Acc^3]AVP it is considerably reduced. This phenomenon leads to the conclusions that the oxygen atom of the C=O unit of the Gln and/or Asn side chains is involved in the

strong adsorption of the former three peptides on the silver surface, while this interaction for [Cpa^1,Acc^3]AVP is weaker than for others. These conclusions are supported by the enhancement of the C—C=O stretching vibrations, ν(C—C=O), at 923–937 cm^{-1} (see Table III for detailed frequencies).

An additional band at 790, 795, and 796 cm^{-1} occurring in the [Acc^2,D-Arg^8]AVP, [Acc^3]AVP, and [Cpa^1,Acc^3]AVP SERS spectra, respectively, due to the cyclohexane ring vibrations of Acc or/and Cpa, points out that the hexamembered ring assists in the adsorption process of these peptides on the silver surface. The intensity of this band decreases in order of [Acc^2,D-Arg^8]AVP, [Acc^3]AVP, and [Cpa^1,Acc^3]AVP, again suggesting a decrease in the strength of the interaction between Acc/Cpa and Ag (a different distance of the cyclohexane ring from the silver surface) and an increasing rigidity of the structure in the same directions. However, on the basis of a single enhanced band of this molecular fragment it is difficult to confirm this hypothesis.

In the SERS spectra of all peptides investigated in this work, the amide I band is obscured by the bands arising from the aromatic rings as well as ν(C—O) and $\delta(NH_2)$ vibrations. The amide III and the IR-active amide II vibrations are enhanced at $\sim$1279 cm^{-1} and around 1524–1542 cm^{-1}, respectively, in all SERS spectra.

CONCLUSION

It is known that the [Arg^8]vasopressin and its analogues with Tyr at position 2, i.e., [Acc^3]AVP and [Cpa^1,Acc^3]AVP, show different activities. The [Acc^3]AVP turned out to be a V_1 agonist, while [Cpa^1,Acc^3]AVP does not display this property. We postulate that the orientation of the Tyr side chain with regard to the silver surface determine the selectivity of these peptides.

A comparison of the SERS spectra of AVP and its modified analogues [Acc^2,D-Arg^8]AVP, [Acc^3]AVP, and [Cpa^1,Acc^3]AVP shows that the oxygen atom of Tyr in [Cpa^1,Acc^3]AVP interacts slightly with the colloidal silver surface, while there is almost no interaction in the case of the other three peptides. Additionally, we show that the aromatic ring of Phe slightly binds to the silver surface for AVP and [Acc^2,D-Arg^8]AVP. However, in the case of [Acc^2,D-Arg^8]AVP, this interaction is considerably weaker, probably due either to a longer distance between the aromatic ring of Phe and the silver surface or to an almost parallel orientation of the Phe ring on the metal surface. The intensity of the 790–796-cm^{-1} band of the cyclohexane ring in the SERS spectrum of [Acc^3]AVP indicates that the Acc residue is involved in the adsorption process and, similarly to Phe in [Acc^2,D-Arg^8]AVP, it is slightly titled to the surface.

We have demonstrated beyond any doubts that all peptides investigated in this work adsorb on the silver surface via the sulfur atom(s) of the disulfide bridge and the oxygen atom of the Gln and/or Asn C=O moiety. However, the C=O adsorption is less effective for [Cpa^1,Acc^3]AVP than for the other three peptides. The appearance of the $\rho_t(NH_2)$ bands and the reduced intensity of the ν(C=O) band in the SERS spectrum of [Cpa^1,Acc^3]AVP also suggest that Gln or Asn are bound to the surface through both the amide and carbonyl groups of side chains.

Part of this work was supported by internal Jagiellonian University grant WChUJ/DS/05/2004 (to LMP).

REFERENCES

1. Larive, C. K.; Guerra, L.; Rabenstein, D. L. J Am Chem Soc 1992, 114, 7331.
2. Hlavacek, J. Handbook of Neurohyphophyseal Hormone Analogs; Joşt, K., Lebl, M., Brtnik, F., Eds.; CRC Press: Boca Raton, FL, 1987; Vol 1, p 109.
3. Langs, D. A.; Smith, G. D.; Stezowski, J. J.; Hughes, R. E. Science 1986, 232, 1240.
4. Hempel, J. C. The Peptides: Analysis, Synthesis, Biology; Smith, C. W., Ed.; Academic Press: New York, 1987; Vol 8, p 209.
5. Hruby, V. J.; Lebl, M. I. CRC Handbook of Neurohypophyseal Hormone Analogs; Jost, K., Lebl, M., Brtnik, F., Eds.; CRC Press: Boca Raton, FL, 1987; Vol. 1, p 105.
6. Schmidt, J. M.; Ohlenschläger, O.; Rüterjans, H.; Grzonka, Z.; Kojro, E.; Pavo, I.; Fahrenholz, F. Eur J Biochem 1991, 201, 355.
7. Liwo, A.; Tempczyk, A.; Oldziej, S.; Shenderovich, M. D.; Hruby, V. J.; Talluri, S.; Ciarkowski, J.; Kasprzykowski, F.; Łankiewicz, L.; Grzonka, Z. Biopolymers 1995, 38, 157.
8. Kaźmierkiewicz, R.; Czapiewski, C.; Lammek, B.; Ciarkowski, J. J Komput Aided Mol Des 1997, 11, 9.
9. Fox, J. A.; Tu, A. T.; Hruby, V. J.; Mosberg, H. I. Arch Biochem Biophys 1981, 211, 628.
10. Carmona, P.; Lasagabaster, A.; Molina, M. Biochim Biophys Acta 1995, 1246, 128.
11. Barth, A.; Zscherp, C. Q Rev Bophys 2002, 35, 369.
12. Podstawka, E.; Ozaki, Y.; Proniewicz, L. M. Appl Spectrosc 2004, 58, 1147.
13. Głowacka, A. E.; Podstawka, E.; Szczęsna-Antczak, M. H.; Kalinowska, H.; Antczak, T. Com Biochem Phys 2005, 140, 321.
14. Efrima, S.; Conway, B. E. Modern Aspects of Electrochemistry; White, R. E., Bockris, J. O'M., Eds.; Plenum Press: New York, 1985; No 16, Chap 4.
15. Chang, R. K. Ber Bunsenges Phys Chem 1987, 19, 296.

16. Jastrzębska, B.; Derdowska, I.; Kowalczyk, W.; Machova, A.; Slaninova, J.; Lammek, B. J Pept Res 2003, 62, 70.
17. Podstawka, E.; Ozaki, Y.; Proniewicz, L. M. Appl Spectrosc 2004, 58, 570.
18. Hruby, V. J.; Deb, K. K.; Fox, J.; Bjarnason, J.; Tu, A. T. J Biol Chem 1987, 253, 6060.
19. Callahan, J. F.; Ashton-Shue, D.; Bryan, H. G.; Bryan, W. M.; Kinter, L. B.; McDonald, J. E.; Moore, M. L.; Schmidt, D. B.; et al. J Med Chem 1989, 32, 391.
20. Smith, D. D.; Slaninova, J.; Hruby, V. J. J Med Chem 1992, 35, 1558.
21. Kosior, M.; Podstawka, E.; Proniewicz, L. M. On the Border of Chemistry and Biology; Koroniak, H., Barciszewski, J., Eds.; Academic Press UW: Wroclaw, 2004; Vol. XI.
22. Asher, S. A.; Ludwig, M.; Johnson, C. R. J Am Chem Soc 1986, 108, 3186.
23. Rajkumur, B. J. M.; Ramakrishnam, V. Spectrochim Acta Part A 2002, 58, 1923.
24. Yu, N. T.; Jo, B. H.; O'Shea, D. C. Arch Biochem Biophys 1973, 156, 71.
25. Sugeta, H.; Go, A.; Miyazawa, T. Chem Lett 1972, 83.
26. Sugeta, H.; Go, A.; Miyazawa, T. Bull Chem Soc Jpn 1973, 46, 3407.
27. Podstawka, E.; Ozaki, Y.; Proniewicz, L. M. Appl Spectrosc 2004, 58, 580.
28. Qian, W.; Krimm, S. J Raman Spectrosc 1992, 23, 517.
29. Harada, I.; Takeuchi, H. In Spectroscopy of Biological Systems; Clark, R. J. H., Hester, R. E., Eds.; John Wiley and Sons: Chichester, 1986; Vol. 13, Chap. 3, p 113.
30. Tu, A. T.; Lee, J.; Deb, K. K.; Hruby, V. J. J Biol Chem 1979, 254, 3272.
31. Haris, P. I.; Severcan, F. J Mol Catal B 1999, 7, 207.
32. Kendrick, B. S.; Meyer, J. D.; Matsuura, J. E.; Carpenter, J. F.; Manning, M. C. Arch Biochem Biophys 1997, 347, 113.
33. Surewicz, W. K.; Mantsch, H. H.; Chapman, D. Biochemistry 1993, 32, 299.
34. DePaz, R. A.; Dale, D. A.; Barnett, Ch. C.; Carpenter, J. F.; Gertner, A. L.; Randolph, T. W. Enzyme Mikrob Tech 2002, 31, 765.
35. Tu, A. T. Spectros Biol Syst 1986, 13, 47.
36. Ngarize, S.; Herman, H.; Adams, A.; Howell, N. J Agricul Food Chem 2004, 52, 6470.
37. Olinger, J. M.; Ill, D. N.; Jakobsen, R. J.; Brody, R. S. Biochim Biophys Acta 1986, 869, 89.
38. Surewicz, W. K.; Mantsch, H. H. Biochim Biophys Acta 1988, 952, 115.
39. Byler, D. M.; Susi, H. Biochim Biophys Acta 1986, 25, 469.
40. Herne, T. M.; Ahern, A. M.; Garrell, R. L. J Am Chem Soc 1991, 113, 846.
41. Stewart, S.; Fredericks, P. M. Spectrochim Acta Part A 1999, 55, 1641.
42. Suh, J. S.; Moskowits, M. J Am Chem Soc 1986, 108, 4711.
43. Ooka, A. A.; Garell, R. L. Biopolymers 2000, 57, 92.
44. Podstawka, E.; Borszowska, R.; Grabowska, M.; Drąg, P.; Kafarski, M.; Proniewicz, L. M. Surf Sci 2005, 599, 207.
45. Castro, J. L.; Lopez Ramirez, M. R.; Lopez Tocon, I.; Otero, J. C. J. Colloid Interf Sci 2003, 263, 357.
46. Nabiev, I. R.; Savchenko, V. A.; Efremov, E. S. J Raman Spectrosc 1983, 14, 375.
47. Joo, S. W.; Han, S. W.; Kim, K. J Phys Chem B 1999, 103, 10831.
48. Gao, P.; Weaver, M. J. J Phys Chem 1985, 89, 5040.
49. Podstawka, E.; Kozłowski, H.; Proniewicz, L. M. J Raman Spectrosc 2006, 37, 574.
50. Moskovits, M. Rev Modern Phys 1985, 57, 783.
51. Moskovits, M.; Suh, J. S. J Phys Chem 1984, 88, 5526.
52. Yim, Y. H.; Kim, K.; Kim, M. S. J Phys Chem 1990, 94, 2552.

Reviewing Editor: George J. Thomas